Inorganic Chemistry

ARTICLE

pubs.acs.org/IC

On the Formation of "Hypercoordinated" Uranyl Complexes

George Schoendorff,[†] Wibe A. de Jong,[‡] Michael J. Van Stipdonk,[§] John K. Gibson,[∥] Daniel Rios,[∥] Mark S. Gordon,[†] and Theresa L. Windus*[,†]

[†]Department of Chemistry, Iowa State University and Ames Laboratory, Ames, Iowa 50011, United States

[‡]Environmental Molecular Sciences Laboratory, Pacific Northwest National Laboratory, P.O. Box 999, Richland, Washington 99352, United States

[§]Department of Chemistry, Wichita State University, Wichita, Kansas 67260-0051, United States

[∥]Chemical Sciences Division, The Glenn T. Seaborg Center, Lawrence Berkeley National Laboratory, Berkeley, California 94720, United States

Supporting Information

ABSTRACT: Recent gas-phase experimental studies suggest the presence of hypercoordinated uranyl complexes. Coordination of acetone (Ace) to uranyl to form hypercoordinated species is examined using density functional theory (DFT) with a range of functionals and second-order perturbation theory (MP2). Complexes with up to eight acetones were studied. It is shown that no more than six acetones can bind directly to uranium and that the observed uranyl complexes are not hypercoordinated. In addition, other more exotic species involving proton transfer between acetones and species involving enol tautomers of acetone are high-energy species that are unlikely to form.

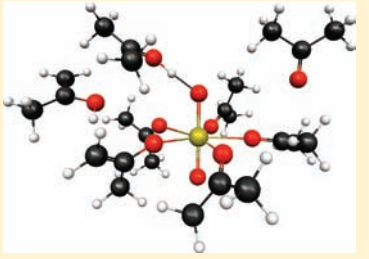

INTRODUCTION

Actinide chemistry is essential to the development of technologies related to nuclear power and nuclear waste management and speciation. Of particular interest is the chemistry of the early actinides, Th through Am, and hexavalent actinyl ions $[O{=}An{=}O]^{2+}$ are frequent subjects of study, especially the uranyl dication (UO_2^{2+}). Uranyl dication coordinated with up to five acetone ligands has been experimentally observed in the gas phase.[1] Density functional theory (DFT) has been used to study the formation of dicationic uranyl complexes with acetone and predicts stable species with up to six acetone ligands in the gas phase.[2] A recent experimental study has verified the existence of the hexacoordinated uranyl species and suggests hypercoordinated species with up to eight acetones.[3] Possible mechanisms for the binding of the seventh and eighth acetones are examined in the present work as well as a comparison of the binding energies obtained using various DFT functionals and second-order perturbation theory (MP2). The choice of initial structures was based on the mechanisms proposed in ref 2.

METHODS

All calculations were performed using the NWChem software suite.[4,5] The choice of functional and basis set used for structure optimizations was based on a previous systematic study in which fully relativistic coupled cluster theory (four-component CCSD(T)) benchmark calculations on UO_2^{2+} were compared to various levels of theory, DFT functionals, and basis set choices.[6] That study showed that the best agreement using DFT was obtained with the local density approximation (LDA)[7,8] to determine optimized structures and Hessians and the B3LYP[9,10] functional at the LDA-optimized structures for energies. MP2 also performed well in the benchmark study, but the computational cost is an order of magnitude greater than it is for the DFT functionals that were used. Accordingly, all structure optimizations and Hessians were obtained using LDA, and all energies reported were obtained with the B3LYP functional using the LDA-optimized structure. Since long-range effects may be important in structures with ligands in the second solvation shell of UO_2^{2+}, binding energies were also calculated using the B2PLYP,[11] CAM-B3LYP,[12] and SSB-D[13,14] functionals at the LDA-optimized structures. These functionals were chosen because they are the most commonly used to address long-range effects. MP2 binding energies are also reported to provide an ab initio method that includes electron correlation for comparison. All reported energies include the vibrational zero-point energy correction.

The small core Stuttgart relativistic effective core potential (RECP) and associated Stuttgart orbital basis set[15−17] were employed for uranium, while valence triple-ζ plus polarization (TZVP)[18] DFT-optimized basis sets were used for all other atoms (H, C, and O). In all cases, spherical Gaussian functions were used. Molecular images were produced using MacMolPlt.[19]

RESULTS

Complexes of acetone coordinated to dicationic uranyl have been studied previously for systems involving up to six acetone ligands.[2] Table 1 contains the binding energies for first five acetone additions. The values of the binding energies obtained with the B3LYP functional have been previously reported along

Received: May 21, 2011
Published: August 08, 2011

with a description of the bonding for each of the complexes.[2] This earlier study indicated evidence of donation of electron density into the empty f orbitals with some degree of back-bonding into the π^* orbitals on the carbonyl group. However, a Mulliken charge analysis indicated that the primary bonding interaction in these complexes is driven by electrostatics. As ligands are added to uranyl, the +2 charge of the system is spread out into the ligands. Thus, for the first addition, significant charge is shifted to the acetone. As subsequent ligands are added, the amount of charge on each ligand becomes less until there are essentially no additional changes in the charge distribution with additional ligands. The energies of these structures have been recalculated using the B2PLYP, CAM-B3LYP, and SSB-D functionals as well as MP2 (Table 1). In general, the binding energies decrease with increasing coordination number. Even though the general trend is correct, both LDA and B2PLYP significantly overbind the first acetone addition. B2PLYP continues to overbind for the next two acetone additions. LDA also overbinds all of the subsequent acetone additions. Accordingly, while LDA can provide reasonable structures, the relative energies of these complexes are not reliable when the LDA functional is used. The fact that LDA overbinds is well known, but the overbinding observed for the B2PLYP functional is in excess of values generally reported.[20,21] However, existing benchmark studies on the quality of DFT functionals frequently neglect molecules containing actinides. The origins of the rather drastic overbinding of the first acetone for LDA and B2PLYP are unknown.

The remaining functionals, B3LYP, CAM-B3LYP, and SSB-D, yield binding energies that are in much closer agreement with MP2 than either LDA or B2PLYP for 1−3 ligands. While the trend in the B3LYP binding energies is the same as MP2, B3LYP tends to underbind the ligands. The CAM-B3LYP functional tends to be more binding than B3LYP, and the SSB-D functional matches the MP2 binding energies better than any of the other functionals examined. It was expected that the CAM-B3LYP and SSB-D functionals could continue to provide energies that closely agree with MP2 when additional acetones are added to the system due to their ability to account for long-range interactions. The difference in binding energies between B3LYP and CAM-B3LYP is primarily the result of how the functional includes HF exchange. The HF contribution to CAM-B3LYP is local and varies from one region of the molecule to another, while B3LYP employs a "global" HF contribution that is not dependent on position.[22]

Table 1. Binding Energies (kcal/mol) for the First Five Acetone Additions Including Zero-Point Energy[a]

	DFT					
no. of acetones	LDA	B2PLYP	B3LYP[2]	CAM-B3LYP	SSB-D	MP2
1	−730.7	−813.8	−108.1	−107.3	−110.3	−177.7
2	−87.8	−76.2	−75.0	−76.7	−72.4	−72.3
3	−66.7	−60.1	−57.8	−60.2	−54.5	−49.5
4	−46.9	−35.5	−30.8	−34.4	−37.0	−37.0
5	−29.6	−19.9	−12.7	−17.3	−21.5	−26.3

[a] Binding energies are computed for the reactions $[UO_2(Ace)_{n-1}]^{2+}$ + Ace → $[UO_2(Ace)_n]^{2+}$.

Uranyl complexes with six acetones are shown in Figure 1. Complex **1A** has all six acetone ligands bound directly to uranyl, while complex **1B** has five acetone ligands bound directly to uranyl with the sixth acetone in the second solvation sphere. The sixth acetone in complex **1A** is directly bound to the metal center through a uranium−oxygen interaction, while in complex **1B** it is bound noncovalently to two of the acetone ligands on uranyl.

Uranyl complexes with seven bound species are shown in Figure 2. Structure **2A** optimized to a complex with six acetones occupying equatorial sites on uranyl with the seventh acetone in the second solvation shell. Structure **2B** is a five-coordinate complex with two acetones in the second solvation shell. Additional species consistent with the experimental results have been proposed that involve proton transfer between acetones as well as complexes involving acetone as the enol tautomer.[3] Complex **2C** has five acetone ligands bound directly to uranyl in the equatorial positions. A sixth equatorial ligand is a deprotonated acetone. The proton from this ligand has been transferred to the seventh acetone to produce an alcohol. This alcohol is bound via a hydrogen bond to one of the axial oxygens from uranyl. The final complex with seven acetones involves the enol tautomer of acetone. As with complex **2C**, complex **2D** involves a hydrogen-bonding interaction between an axial oxygen from uranyl and the alcohol hydrogen from the enol tautomer of acetone. The remaining six acetones are directly bound to equatorial positions on uranyl.

Optimized structures of complexes containing eight bound species are presented in Figure 3. Structure **3A** has five acetones bound directly to uranyl in the equatorial plane. The remaining three acetones are not directly bound to uranyl and lie above the equatorial plane. Structure **3B** has four acetone ligands directly bound to uranyl. The fifth equatorial coordination site is occupied by a deprotonated acetone. One protonated acetone is bound via a hydrogen bond to one of the axial oxygens from uranyl. One

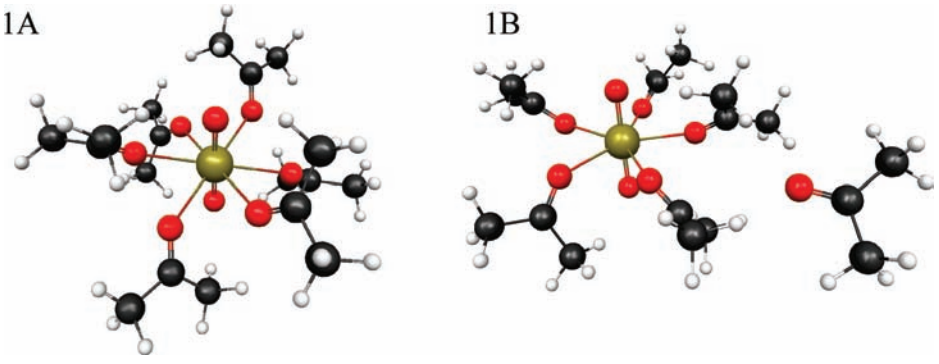

Figure 1. Complexes of UO_2^{2+} with six acetones. Complex **1A** has six acetone ligands directly bound to uranyl, and complex **1B** has five acetone ligands directly bound to uranyl with the sixth acetone in the second solvation sphere.

dx.doi.org/10.1021/ic201080z |*Inorg. Chem.* 2011, 50, 8490–8493

enol tautomer of acetone is in the second solvation shell between the deprotonated ligand and the hydrogen-bonded protonated acetone (far left of **3B**). The final acetone is in the second solvation shell. Structure **3C** has six acetones directly bound to uranyl with enol tautomers of acetone bound via hydrogen bonds to each of the axial oxygens on uranyl.

Table 2 shows the binding energies for the complexes containing six, seven, and eight acetones for the various functionals employed and compares them with the MP2 binding energies. Binding energies for the complexes with seven acetones are calculated with the precursors **1A** and **1B** (values from **1B** are in parentheses). MP2 and LDA both predict complex **1A** to be the more stable product by approximately 3 kcal/mol, while the B2PLYP, B3LYP, CAM-B3LYP, and SSB-D functionals all show complex **1B** to be lower in energy. The difference in energy between complexes **1A** and **1B** is 7.6 kcal/mol or less at all levels of theory with the B3LYP functional producing the largest energy difference. At the fifth acetone addition, uranyl is nearly saturated and addition of a sixth ligand leads to weak binding. Thus, the difference in energy for a six-coordinate complex versus a five-coordinate complex with one acetone in the second solvation sphere will be small. For complexes with seven or more acetones, LDA binding energies differ significantly from the MP2 binding energies. B2PLYP is in much closer agreement with MP2 for the large species, but the deviation from MP2 remains unpredictable (significantly overbinding in some cases and underbinding in others). The remaining functionals also do not perform well compared with MP2. In some cases the DFT binding energy sign differs from the MP2 sign (for example, **2A** and **2C** binding energies for SSB-D vs MP2). Furthermore, the lowest vibrational frequencies predicted for each of these structures ranges from 6cm^{-1} (**3B**) to 20 cm^{-1} (**2B**). Since the LDA Hessian for each of these structures is positive definite, they are all shallow minima on the LDA potential energy surface. This indicates that these are floppy, weakly bound structures. If each structure in Table 2 that has a positive binding energy is optimized using the corresponding method, these species may spontaneously dissociate. Because these structures exist in shallow minima, there may be

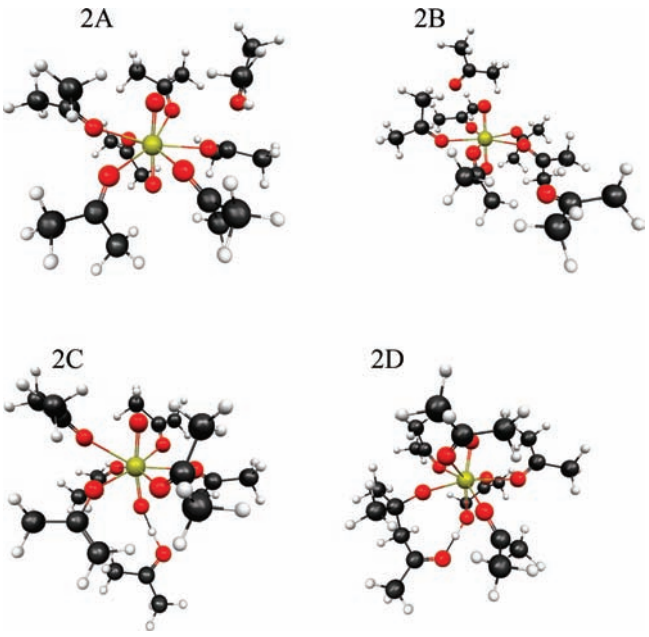

Figure 2. Complexes of UO_2^{2+} with seven bound species. Complexes **2A** and **2B** have seven acetones, complex **2C** involves proton transfer between acetone ligands, and complex **2D** has an enol tautomer of acetone bound to an axial oxygen from uranyl via a hydrogen bond.

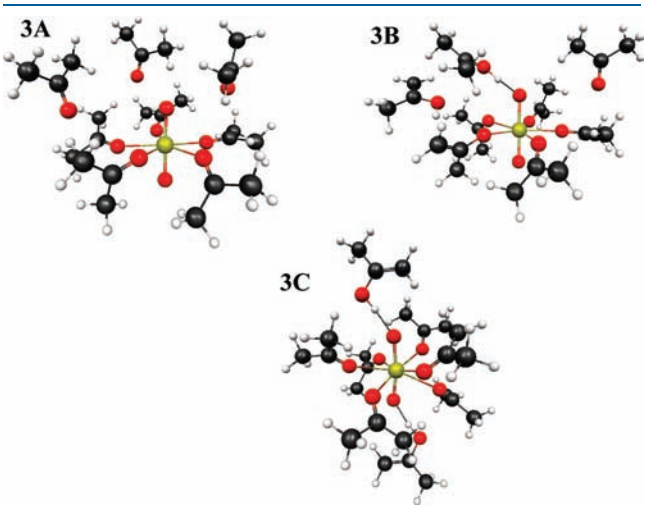

Figure 3. Complexes of UO_2^{2+} with eight bound species. Complex **3A** has eight acetones, complex **3B** involves proton transfer between acetones and one enol tautomer, and complex **3C** has two enol tautomers of acetone bound to the axial oxygens from uranyl via hydrogen bonds.

Table 2. Binding Energies (kcal/mol) for Addition of the Sixth, Seventh, and Eighth Acetone Additions[a]

	DFT					
	LDA	B2PLYP	B3LYP	CAM-B3LYP	SSB-D	MP2
1A	−25.0	−9.9	−3.9	−7.5	−10.5	−8.6
1B	−22.3	−13.9	−11.5	−13.6	−17.4	−5.9
2A	−8.1 (−10.9)	2.3 (6.3)	7.8 (15.3)	4.6 (10.7)	−4.7 (2.1)	2.1 (−0.6)
2B	−13.4 (−16.1)	−8.6 (−4.6)	−8.1 (−0.5)	−9.4 (−3.3)	−15.4 (−8.5)	−3.3 (−6.0)
2C	−5.6 (−8.7)	16.4 (20.4)	17.1 (27.9)	14.0 (27.8)	−0.1 (18.6)	4.5 (16.8)
2D	−20.2 (−22.9)	7.6 (11.6)	20.4 (24.7)	21.7 (20.0)	11.8 (6.7)	19.5 (1.8)
3A	−12.1	−6.1	−1.3	−5.6	−11.5	−5.1
3B	−1.3	26.6	36.3	34.9	28.4	32.3
3C	2.9	31.5	−0.7	29.0	21.1	28.9

[a] Binding energies are computed for the reactions $[UO_2(Ace)_5]^{2+}$ + Ace → {**1A**, **1B**}, **1A** or (**1B**) + Ace → {**2A**, **2B**, **2C**, or **2D**}, and **2B** + Ace → {**3A**, **3B**, or **3C**}. The binding energies in parentheses are from acetone additions to **1B**. All binding energies include the zero-point energy correction.

dx.doi.org/10.1021/ic201080z |*Inorg. Chem.* 2011, 50, 8490–8493

other local minima on the potential energy surface with comparable energies.

CONCLUSIONS

There are some important details that can be elucidated from the data presented here. It has been shown that care must be taken when choosing a density functional for these systems. The results of this study suggest that the SSB-D functional provides the best binding energies compared with MP2 for complexes that have acetone directly bound to uranyl, and CAM-B3LYP provides the best agreement with MP2 for complexes that have acetones that are not directly bound to uranyl. With six acetones, only LDA gave the correct trend (although it significantly overbinds compared to MP2).

More significantly, the hypercoordinated species previously reported[3] do not simply involve coordination of acetone ligands to uranyl. The seventh and eighth and in some computational approaches even the sixth acetones generally do not bind directly to uranyl. There simply is not sufficient room in the equatorial plane to accommodate so many bulky ligands. However, the structures with additional acetones in the second solvation sphere do appear to be possible from the binding energies. Other more exotic species involving proton transfer between acetones and species involving enol tautomers of acetone are high-energy species that are unlikely to form. Additionally, the complexes obtained exist in very shallow potential energy wells, suggesting that numerous geometries might be possible, although the last few acetones will necessarily be in the second solvation shell.

The experimental conditions under which the apparently "hypercoordinated" complexes, $[UO_2(Ace)_{6,7,8}]^{2+}$, were observed have been described.[3] An ion trap gas-phase hydration study under similar conditions resulted in monopositive metal-ion complexes coordinated by inner-shell waters but not second-shell waters.[23] DFT computations of $[Yb(OH)_2(H_2O)_n]^+$ (n = 1−5), for example, demonstrated that the first four waters are directly bound to the Yb metal center. Addition of a fifth water to the second shell was computed to be both exothermic and exoergic but was not observed under the experimental conditions, $P[H_2O] \approx 10^{-6}$ Torr H_2O and $T \approx 300$ K. As second-shell acetones should generally be less strongly bound than hydrogen-bonded second-shell waters and the acetone pressure in the ion trap is less than that of water, experimental observations of weakly bound second-shell acetones such as in structure **3A** are not expected. From the experimental observation of the $[UO_2(Ace)_{6,7,8}]^{2+}$ complexes and the theory results that their energetically favored structures have outer-sphere acetones, it can be concluded that the observed complexes most probably do not comprise only acetone ligands and that uranyl is not necessarily "hypercoordinated". Among alternative ligands that will be considered in future theory and experimental studies of these enigmatic complexes is diacetone alcohol, $CH_3C(O)CH_2C(OH)(CH_3)_2$, which is an acetone dimer that is not readily discernible from two acetones by simple mass spectrometry.

ASSOCIATED CONTENT

Supporting Information. Atomic coordinates for optimized structures, absolute energies, and zero-point energies. This material is available free of charge via the Internet at http://pubs.acs.org.

AUTHOR INFORMATION

Corresponding Author
*E-mail: twindus@iastate.edu.

ACKNOWLEDGMENT

This research was performed in part using the Molecular Science Computing Facility (MSCF) in the William R. Wiley Environmental Molecular Sciences Laboratory, a National scientific user facility sponsored by the U.S. Department of Energy's Office of Biological and Environmental Research and located at the Pacific Northwest National Laboratory, operated for the Department of Energy by Battelle. Funding has been provided by Iowa State University and an NSF grant for petascale applications. W.d.J.'s, J.K.G.'s, and D.R.'s work was supported by the BES Heavy Element Chemistry program of the U.S. Department of Energy, Office of Science. Work at LBNL was supported by the Director, Office of Science, Office of Basic Energy Sciences, Division of Chemical Sciences, Geosciences and Biosciences of the U.S. Department of Energy, under Contract No. DE-AC02-05CH11231.

REFERENCES

(1) Van Stipdonk, M. J.; Chien, W.; Anbalagan, V.; Bulleigh, K.; Hanna, D.; Groenewold, G. S. *J. Phys. Chem. A* **2004**, *108*, 10448.
(2) Schoendorff, G.; Windus, T. L.; de Jong, W. A. *J. Phys. Chem. A* **2009**, *113*, 12525.
(3) Rios, D.; Rutkowski, P. X.; Van Stipdonk, M. J.; Gibson, J. K. *Inorg. Chem.* **2011**, *50*, 4781.
(4) Valiev, M.; Bylaska, E. J.; Govind, N.; Kowalski, K.; Straatsma, T. P.; van Dam, H. H. J.; Wang, D.; Nieplocha, J.; Apra, E.; Windus, T. L.; de Jong, W. A. *Comput. Phys. Commun.* **2010**, *181*, 1477.
(5) Kendall, R. A.; Aprà, E.; Bernholdt, D. E.; Bylaska, E. J.; Dupuis, M.; Fann, G. I.; Harrison, R. J.; Ju, J.; Nichols, J. A.; Nieplocha, J.; Straatsma, T. P.; Windus, T. L.; Wong, A. T. *Comput. Phys. Commun.* **2000**, *128*, 260.
(6) de Jong, W. A.; Harrison, R. J.; Nichols, J. A.; Dixon, D. A. *Theor. Chem. Acc.* **2001**, *107*, 22.
(7) Slater, J. C. *Phys. Rev.* **1951**, *81* (3), 1287.
(8) Vosko, S. H.; Wilk, L.; Nusiar, M. *Can. J. Phys.* **1980**, *58* (8), 1200.
(9) Becke, A. D. *J. Chem. Phys.* **1993**, *98*, 5648.
(10) Lee, C.; Yang, W.; Parr, R. G. *Phys. Rev. B* **1988**, *37*, 785.
(11) Grimme, S. *J. Chem. Phys.* **2006**, *124*, 034108.
(12) Yanai, T.; Tew, D.; Handy, N. *Chem. Phys. Lett.* **2004**, *393*, 51.
(13) Swart, M.; Solà, M.; Bickelhaupt, F. M. *J. Chem. Phys.* **2009**, *131*, 094103.
(14) Swart, M.; Solà, M.; Bickelhaupt, F. M. *J. Comput. Methods Sci. Eng.* **2009**, *9*, 69.
(15) Bergner, A.; Dolg, M.; Küchle, W.; Stoll, H.; Preuss, H. *Mol. Phys.* **1993**, *80* (6), 1431.
(16) Küchle, W.; Dolg, M.; Stoll, H. *Mol. Phys.* **1991**, *74* (6), 1245.
(17) Küchle, W.; Dolg, M.; Stoll, H.; Preuss, H. *J. Chem. Phys.* **1994**, *100* (10), 7535.
(18) Godbout, N.; Salahub, D. R.; Andzelm, J.; Wimmer, E. *Can. J. Chem.* **1992**, *70* (2), 560.
(19) Bode, B. M.; Gordon, M. S. *J. Mol. Graphics Modell.* **1998**, *16*, 133.
(20) Goerigk, L.; Grimme, S. *Phys. Chem. Chem. Phys.* **2011**, *13*, 6670.
(21) Karton, A.; Daon, S.; Martin, J. M. L. *Chem. Phys. Lett.* **2011**, *510*, 165.
(22) Akinaga, Y.; Ten-no, S. *Chem. Phys. Lett.* **2008**, *462*, 348.
(23) Rutkowski, P. X.; Michelini, M. C.; Bray, T. H.; Russo, N.; Marçalo, J.; Gibson, J. K. *Theor. Chem. Acc.* **2011**, *129*, 575.